Load Prediction-based Energy-efficient Hydraulic Actuation of a Robotic Arm

Miss Can Du, Prof Andrew Plummer and Dr Nigel Johnston

Centre for Power Transmission and Motion Control
University of Bath, UK
C.Du@bath.ac.uk

Centre for Power Transmission and Motion Control
University of Bath, UK
A.R.Plummer@bath.ac.uk

Centre for Power Transmission and Motion Control
University of Bath, UK
D.N.Johnston@bath.ac.uk

In this paper the motion of a two-joint robotic arm is controlled by a variable supply-pressure valve-controlled (VPVC) hydraulic system. It has a fixed capacity pump driven by a brushless servo-motor. The minimum required supply-pressure for the demand motion is predicted. It is computed from the predicted piston force, by applying Lagrange's equations of the-second-kind. The supply-pressure for the whole system is the higher one of the two load branches; the other branch is controlled by throttling. The supply-pressure is varied by controlling motor speed. Simulated and experimental results are shown and discussed. A power consumption comparison with fixed supply-pressure system shows up to 73% saving is found experimentally.

Keywords: Load prediction, energy-efficiency, hydraulic actuation, motion control
Target audience: Control System Designers

1 Introduction

In many hydraulic applications, energy efficiency is becoming an important consideration. For a system with multi load branches, one approach is to generate minimum fluid power from the pump: minimum supply pressure or minimum supply flow [1, 2, and 3]. Pump flow should meet exactly the total flow demand with the help of an electronic controller [1]. A method named flow control with indirect feedback was illustrated by Djurovic and Helduser [2]. One primary pressure compensator (PC) instead of a flow sensor is used in each actuator. The method observes whether pump flow is excessive or insufficient via the opening of the PC. A novel power management algorithm for electronic load sensing (ELS) on a telehandler is introduced in [3]. This new ELS algorithm can achieve the advantages of a hydro-mechanical load sensing system: pressure control, flow-sharing, anti-stall, power sharing and prioritization of steering, in the meantime, it can take into account dynamic performance with a load sensing-margin down to 7 bar.

In this paper, a variable pressure valve controlled (VPVC) hydraulic actuation system will be illustrated. It is a hydraulic plant which aims to reduce energy loss by generating a variable supply pressure (P_S). The main idea of the VPVC algorithm is to estimate the minimum P_S required in advance, thus improving dynamic response. It is similar to load sensing but it does not use any actual pressure signals for control. It predicts the force required by the actuators thus estimating the P_S. In addition, it adopts an electronic controller and a servo motor to drive a fixed displacement pump. This can reduce the weight of plant compared with the traditional load sensing system with a hydraulic controller and a variable displacement pump [4].

A FPVC (fixed supply pressure valve-controlled) hydraulic actuation system has to throttle the flow by the valve to reduce the pressure, which brings an energy loss across the valve. If there are several load branches, the supply pressure should be high enough for all the load branch requirements and all duty cycles.

Figure 1: The robotic arm

The potential advantages of VPVC are: good efficiency due to variable P_S; lighter than traditional load sensing plants (a small fixed-displacement pump, electronic controller). Hence VPVC is suitable for mobile robotic applications where efficiency and weight are crucial. In this project, a robotic arm with two joints (two linear cylinders to rotate two joints) will be actuated by a VPVC controller. Both simulation and experimental results will be presented.

The prototype robotic arm used in this project is an inverted Robot Leg HyQ-LegV2.1 from the Italian Institute of Technology [1](Figure 1). The hydraulic circuit is shown in Figure 2.

This paper begins with the control algorithm derivation, including modelling required for the model-based controller. The last section is experimentation for FPVC and VPVC, comparing simulated results and experimental results. At the end, a summary of the power consumed by the FPVC and VPVC systems is given.

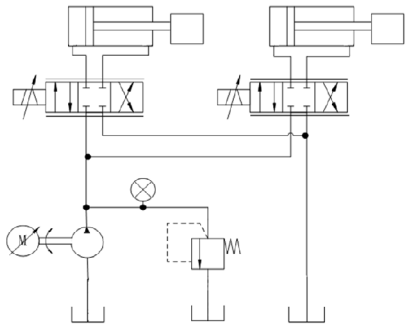

Figure 2: The hydraulic circuit

[1] http://www.iit.it/en/robots/hyq.html

2 Controller

The VPVC control algorithm has two parts: feed forward and feedback.

The feed forward is to predict the required minimum P_S of the system along with the required spool positions of valves. The calculation can be illustrated by the flow chart in Figure 3. The P_S estimated when an individual control valve is fully open is called P_{SO}, and the one to avoid cavitation in the thrust chamber is P_{SC}. P_{SO} and P_{SC} for each actuator are calculated then the actuator with highest required P_S is chosen to be master actuator (MA). Its required P_S is the final P_S of the whole system. The spool position for the other valve should be computed with this P_S. The prediction of P_{SO} and P_{SC} is a crucial problem, which will be discussed in detail in the following section. In this paper, oil compressibility is neglected.

2.1 Supply pressure prediction

2.1.1 Supply pressure required with fully open valve (P_{SO})

During extension, the return line is connected to the rod side chamber P_B and the supply line is connected to the piston side chamber P_A. The flow rate demand can be obtained from $Q_1 = A_1 v$, $Q_2 = A_2 v$; (Q_1 is the flow rate into piston side chamber, and Q_2 is the flow rate out of the rod side chamber.)

The pressure drops across the valve can be represented as follows:

$$\Delta P_{valve\ 1} = P_S - P_A \tag{1}$$

$$\Delta P_{valve\ 2} = P_B - P_R \tag{2}$$

Then the orifice equation gives:

$$Q_1 = K_V x\sqrt{\Delta P_{valve1}} \tag{3}$$

$$Q_2 = K_V x\sqrt{\Delta P_{valve2}} \tag{4}$$

If the valve is fully open i.e. x is 100%, and then from Equation (2) and Equation (4) P_B can be calculated with an assumption of P_R's value and known K_V from the valve's catalogue.

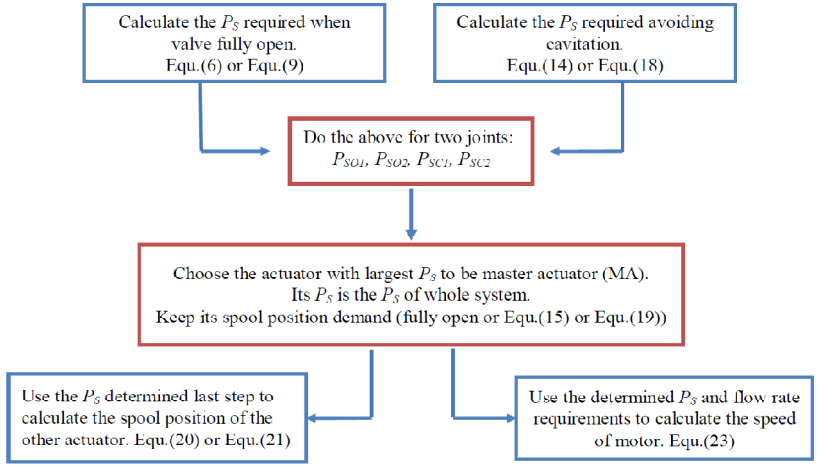

Figure 3: The flow chart of feed forward in VPVC

$$P_A A_1 - P_B A_2 = F \tag{5}$$

From Equation (5) P_A can be evaluated now.

Finally, back to Equation (1) and Equation (3) the required P_S can be estimated.

$$P_{SO} = \frac{(A_1^3 + A_2^3)v^2}{A_1 K_V^2} + \frac{F + A_2 P_R}{A_1} \tag{6}$$

When retracting, the return line is connected to the piston side P_A and the supply line is connected to the rod side chamber P_B.

$$\Delta P_{valve\ 1} = P_A - P_R \tag{7}$$

$$\Delta P_{valve\ 2} = P_S - P_B \tag{8}$$

Then using a similar process as for P_{SO} when extending, the P_S can be predicted:

$$P_{SO} = \frac{(A_1^3 + A_2^3)v^2}{A_2 K_V^2} + \frac{A_1 P_R - F}{A_2} \tag{9}$$

2.1.2 Supply pressure required to avoid cavitation (P_{SC})

When extending, P_S is connected to P_A, which is set to a minimum pressure of P_{th} (in this project, P_{th} = 2 bar).

$$\Delta P_{valve\ 1} = P_S - P_{th} \tag{10}$$

$$\Delta P_{valve\ 2} = P_B - P_R \tag{11}$$

$$\frac{\Delta P_{valve\ 1}}{\Delta P_{valve\ 2}} = \frac{Q_1^2}{Q_2^2} = \frac{A_1^2}{A_2^2} = \alpha^2 \tag{12}$$

With the force equation

$$P_{th} A_1 - P_B A_2 = F \tag{13}$$

The value of P_S can be calculated:

$$P_{SC} = (\alpha^3 + 1)P_{th} - \frac{\alpha^2}{A_2} F - \alpha^2 P_R \tag{14}$$

The corresponding spool position for the valve to control this MA is computed:

$$x = \frac{A_1 v}{K_V \sqrt{P_{SC} - P_{th}}} \tag{15}$$

When retracting, P_S is connected to P_B, which is set to a minimum pressure of P_{th}.

$$\Delta P_{valve\ 1} = P_A - P_R \tag{16}$$

$$\Delta P_{valve\ 2} = P_S - P_{th} \tag{17}$$

Following the same procedure as for P_{SC} when extending, P_S can be predicted:

$$P_{SC} = (\frac{1}{\alpha^3} + 1)P_{th} + \frac{1}{A_1 \alpha^2} F - \frac{P_R}{\alpha^2} \tag{18}$$

The corresponding spool position for the valve to control this MA is computed:

$$x = \frac{A_2 v}{K_V \sqrt{P_{SC} - P_{th}}} \tag{19}$$

The final choice of P_S = max (P_{SO1}, P_{SO2}, P_{SC1}, P_{SC2}), where subscripts 1 and 2 refer to shoulder actuator and elbow actuator respectively. Hence the spool position of the master actuator (MA) is fully open or for cavitation avoidance is given by Equation (15) or Equation (19). The spool position of the other cylinder is computed by the final value of P_S in Equation (20) or Equation (21) below.

2.2 Spool opening of the other cylinder (Non-MA) and motor speed calculation

If the other cylinder is required to extend, its spool opening should be:

$$x_j = \frac{A_2 v_j}{K_V \sqrt{\frac{P_S A_1 - P_R A_2 - F_j}{\alpha^2 A_1 + A_2}}} \tag{20}$$

If the other cylinder is required to retract, its spool opening should be:

$$x_j = \frac{A_1 v_j}{K_V \sqrt{\frac{(P_S A_2 - P_R A_1 + F_j)\alpha^2}{\alpha^2 A_1 + A_2}}} \tag{21}$$

where x_j is the spool position demand of the other cylinder; v_j and F_j are its velocity demand and load force respectively; and the area ratio is defined as: $A_1/A_2 = \alpha$ (22)

When the final P_S is determined, given the desired flow rate of each actuator, the required motor speed $\hat{\omega}_m$ can be found from Equation (23):

$$\hat{\omega}_m = \frac{\frac{d}{dt}\left(\frac{P_S}{K}\right) + \sum_{j=1}^{2} Q_{aj}}{D_P} \tag{23}$$

where K is effective stiffness of the oil inside the supply hoses, and D_P is the displacement of pump.

2.3 Required force prediction

From the last section, it is clear that the required force F is required for the P_S prediction algorithm. The force is derived by Lagrange equation of the second kind, which incorporates inertia and weight related items.

$$\frac{d}{dt}\left(\frac{\partial L}{\partial \dot{\theta}_1}\right) - \frac{\partial L}{\partial \theta_1} = q_1 \tag{24}$$

$$\frac{d}{dt}\left(\frac{\partial L}{\partial \dot{\theta}_2}\right) - \frac{\partial L}{\partial \theta_2} = q_2 \tag{25}$$

where $L = T - V$, L is the Lagrangian of the system; T is the total kinetic energy and V is the total potential energy of the robotic arm. q_1 **and** q_2 are the generalized forces, hence in this case they are the torques required by the shoulder joint and elbow joint respectively. The definitions of θ_1 **and** θ_2 are illustrated in Figure 4.

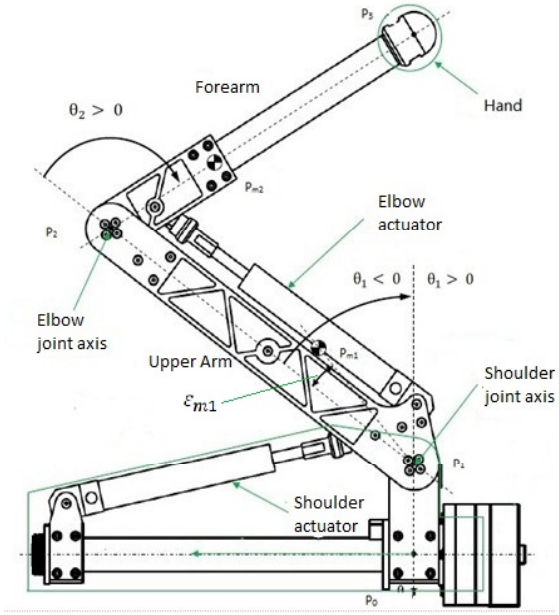

Figure 4: Geometry of the robotic arm

The results of Equation (24) and Equation (25) are as follows:

$$q_1 = (I_1 + I_2 + I_3 + L_1^2 M_2 + L_1^2 M_3 + L_2^2 M_3 + C_1^2 M_1 + C_2^2 M_2)\ddot{\theta}_1 + (I_2 + I_3 + L_2^2 M_3 + C_2^2 M_2)\ddot{\theta}_2 - gL_1(M_2 + M_3)\sin\theta_1 - gM_1 C_1 \sin(\varepsilon_{m1} + \theta_1) - g(L_2 M_3 + C_2 M_2)\sin(\theta_1 + \theta_2) + L_1(L_2 M_3 + C_2 M_2)\left(2\ddot{\theta}_1 + \ddot{\theta}_2\right)\cos\theta_2 - L_1(L_2 M_3 + C_2 M_2)\left(\dot{\theta}_2^{\,2} + 2\dot{\theta}_1\dot{\theta}_2\right)\sin\theta_2 \tag{26}$$

$$q_2 = (I_2 + I_3 + L_2^2 M_3 + C_2^2 M_2)\ddot{\theta}_1 + (I_2 + I_3 + L_2^2 M_3 + C_2^2 M_2)\ddot{\theta}_2 - g(L_2 M_3 + C_2 M_2)\sin(\theta_1 + \theta_2) + L_1(L_2 M_3 + C_2 M_2)\ddot{\theta}_1 \cos\theta_2 + L_1(L_2 M_3 + C_2 M_2)\dot{\theta}_1^{\,2}\sin\theta_2 \tag{27}$$

where:

- M_1 is the mass of upper arm (including elbow cylinder), I_1 is its inertia with respect to upper arm gravity centre, through P_{m1};
- M_2 is the mass of forearm (without hand), I_2 is its inertia with respect to forearm gravity centre, through P_{m2};
- M_3 is the mass of hand, I_3 is its inertia with respect its own gravity centre P_3;
- L_1 is the distance between P_1 and P_2; L_2 is the distance between P_2 and P_3; C_1 is the distance between P_1 and P_{m1}; C_2 is the distance between P_2 and P_{m2}.

The actuator force F required is the value of torque computed divided by a lever arm which varies with angular position. Including a viscous damping force, the required hydraulic force prediction for actuators 1 and 2 is:

$$F_1 = \frac{q_1}{r_1(\theta_1)} + B_1 v_1 \tag{28}$$

$$F_2 = \frac{q_2}{r_2(\theta_2)} + B_2 v_2 \tag{29}$$

where $r_1(\theta_1)$ and $r_2(\theta_2)$ are the actuator level arm lengths, and B_1 and B_2 are the damping viscous coefficients.

2.4 Feedback

The measured positions of the actuators are used for feedback. The circumflex (^) represents the output of the feed forward controller. The tilde (~) represents a command signal.

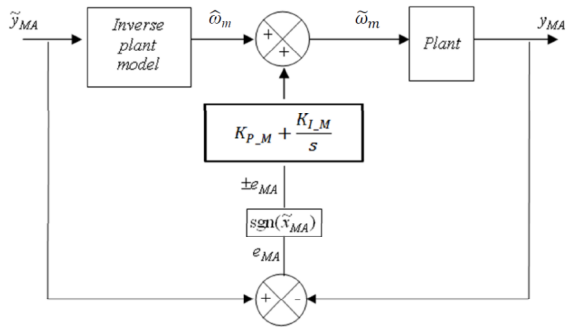

Figure 5: Feedback to motor speed

The position feedback of the MA is used to adjust the motor speed and accordingly the oil flow into the system. There is a proportional-integral (PI) controller multiplied by the sign of MA's spool position (Figure 5). This method takes into account the direction of the flow imposed by the valve. Hence the motor speed command is:

$$\tilde{\omega}_m = \hat{\omega}_m + (K_{P\_M} + \frac{K_{I\_M}}{s})(\tilde{y}_{MA} - y_{MA})sgn(\tilde{x}_{MA}) \quad (30)$$

Actuator position feedback is used to adjust the spool position command of the corresponding valve (Figure 6).

The spool position command is:

$$\tilde{x}_j = \hat{x}_j + (K_{P\_S} + \frac{K_{I\_S}}{s})(\tilde{y}_j - y_j) \quad (31)$$

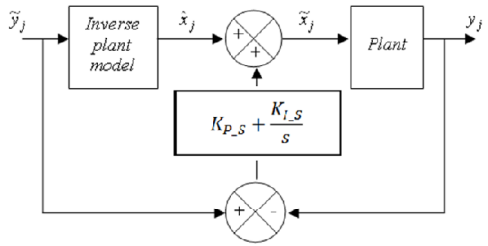

Figure 6: Feedback to actuator spool position

3 Test Rig and Results

3.1 Test rig schematic

The experiments use an xPC Target real time controller and a NI PCI-6221 data acquisition card. The controller sends out a motor speed command and spool position commands. The joint angular positions are sent back to the controller for feedback (Figure 7). A pressure transducer will be used only for supply pressure observation, not for controller. The measured supply pressure will be compared with the simulated signal and predicted pressure.

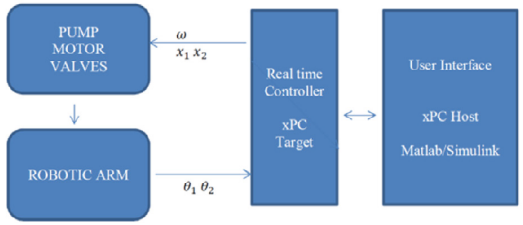

Figure 7: Schematic of test rig

The hydraulic system consists of a servo motor which drives a fixed-displacement piston pump. It uses two direct drive valves to control the flow into the cylinders (Figure 8). The components which are being used are as following:

- Baldor Brushless AC motor BSM63N-375AF: 2.09 Nm continuous, 8.36 Nm peak, 10000 rpm maximum speed;
- Takako micro axial piston pump TFH-315: 3.14 cc/rev, max operating pressure 210 bar, 3000 rpm maximum speed.
- Moog Direct Drive valves D633-R02K01M0NSM2: 5 L/min over 35 bar single path pressure drop.
- Unequal area actuators: 2.01 cm^2/1.23 cm^2

For FPVC experiments, a relief valve and a relatively high motor speed command give a constant supply pressure. Only hydraulic power consumed by cylinders ($Power = Q_{sum\_cylinders}P_S$) are used in power consumption comparison. For VPVC experiments, the relief valve is set at a high cracking pressure.

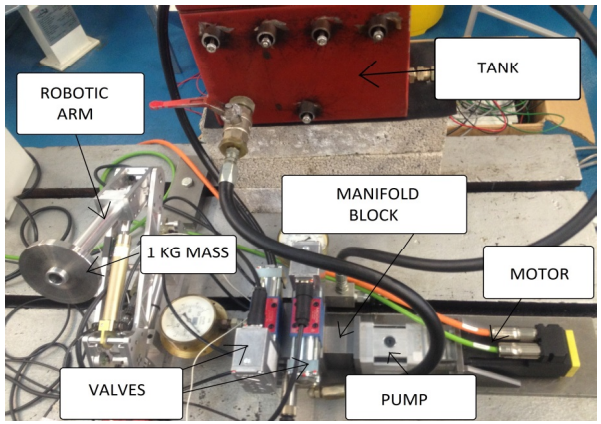

Figure 8: The test rig

3.2 Results (simulation and experimentation)

Before experimentation, corresponding simulated tests with sine wave motion demands have been carried out (Table 1). FPVC uses a constant supply pressure of 39 bar in simulation and experimentation. This is found by observing that the spool positions in simulation should be close to fully open for the most demanding duty cycle.

Test No.	Shoulder Demand	Elbow Demand	FPVC Simulation Information
1	*Amp1* = 20° ω_1 = 3 rad/s	*Amp2* = 20° ω_2 = 4 rad/s	P_S = 39 bar, Max spool opening is 20%
2	*Amp1* = 20° ω_1 = 4 rad/s	*Amp2* = 20° ω_2 = 5 rad/s	P_S = 39 bar, Max spool opening is 35%
3	*Amp1* = 30° ω_1 = 4 rad/s	*Amp2* = 30° ω_2 = 5 rad/s	P_S = 39 bar, Max spool opening is 50%
4	*Amp1* = 20° ω_1 = 7 rad/s	*Amp2* = 30° ω_2 = 6 rad/s	P_S = 39 bar, Max spool opening is 75%
5	*Amp1* = 30° ω_1 = 7 rad/s	*Amp2* = 30° ω_2 = 7 rad/s	P_S = 39 bar, Max spool opening is 98%

Table 1: Tests information

Amp1 and *Amp2* are the amplitudes of sine wave motion demands for shoulder and elbow respectively; ω_1 and ω_2 are corresponding frequencies. For simplicity, only Test 4 (FPVC and VPVC) will be shown and discussed. Note that ω_1 and ω_2 are different frequencies in Test 4.

3.2.1 FPVC results

The position tracking of FPVC (both simulation and experimentation) is shown in Figure 9. The experimental position matches simulated position very well. The supply pressure is fixed at 39 bar. The spool displacement command is shown in Figure 10. The motor speed is commanded to 100 rad/sec i.e. 954 rev/min and is also shown in the figure.

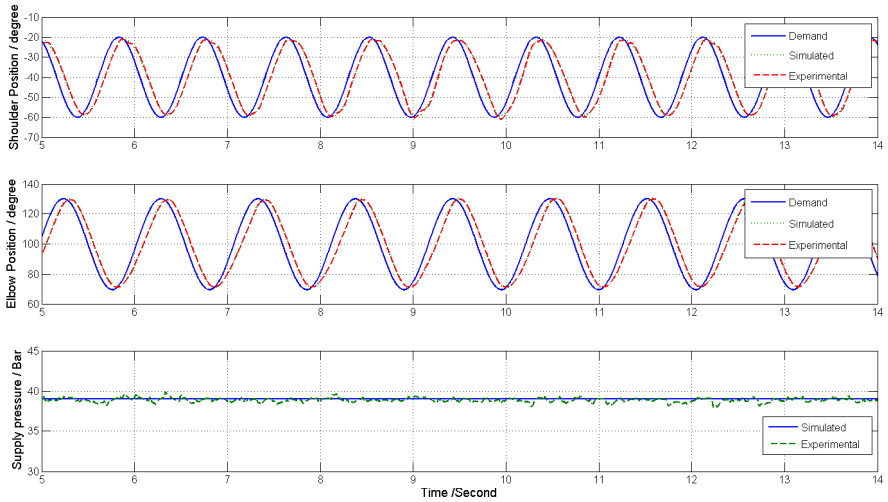

Figure 9: FPVC Test 4 – Angular position tracking and supply pressure tracking

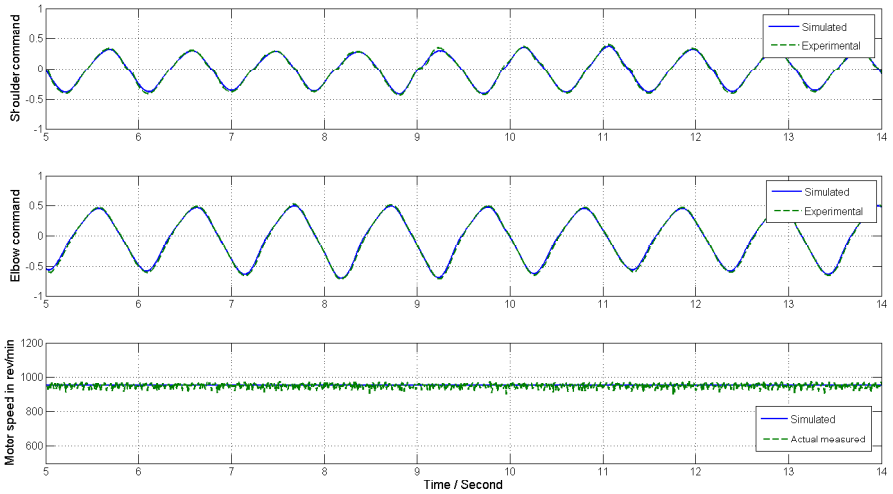

Figure 10: FPVC Test 4 – Valve spool command (-1 to +1) and motor speed

3.2.2 VPVC results

The position tracking and pressure tracking of VPVC is shown (Figure 11). The VPVC control algorithm includes model assumption such as viscous friction, which leads to inevitable errors on hydraulic force prediction, and then on supply pressure prediction. The shoulder motion is slightly affected by elbow motion. But VPVC shows much less lag compared with FPVC position tracking because VPVC predicts the required spool positions while FPVC relies on position feedback control only.

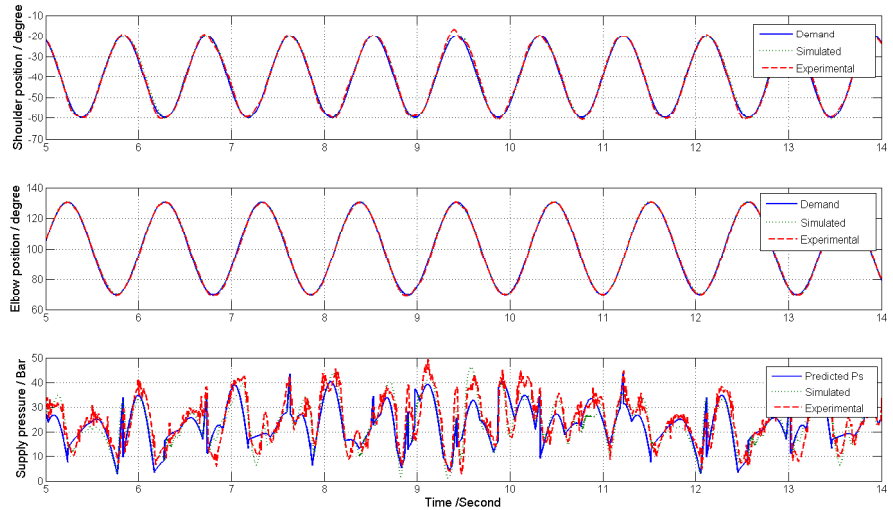

Figure 11: VPVC Test 4 - Angular position tracking and supply pressure tracking

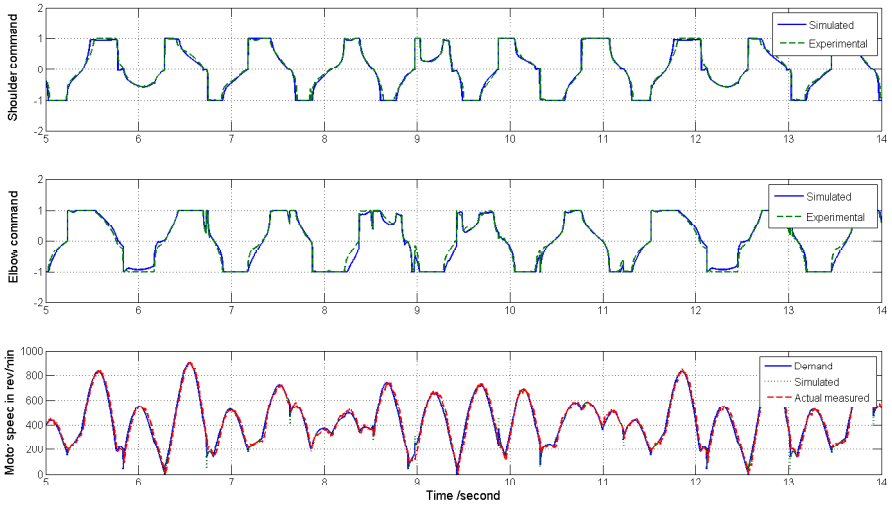

Figure 12: VPVC Test4 –Valve spool command (-1 to +1) and motor speed

The motor speed tracking of VPVC is good (Figure 12). The motor response is very fast with only some transients that the motor cannot track successfully in the experiment (e.g. times 6.73s and 10.32s). In general, the position tracking of VPVC is satisfactory, and experimental pressure tracking and motor speed tracking is good.

3.2.3 Comparison of hydraulic power consumption

The purpose of VPVC is to generate a minimum supply pressure by predicting the force required, and so get a high efficiency compared with a conventional fixed supply pressure system. The hydraulic power of FPVC and VPVC is compared experimentally. The experimental hydraulic power is calculated by velocity (derivative from measured position) and measured supply pressure. The additional power lost through the relief valve with FPVC is not included. From Table 2, it is clear that VPVC can save power among a range of load conditions. The saving increases when the load decreases because FPVC has high waste with low load.

Test No.	FPVC Hydraulic Power (W)		VPVC Hydraulic Power (W)		**Saving (Experimentation)**
	Simulation	**Experimentation**	Simulation	**Experimentation**	
1	38.89	**38.85**	9.31	**10.25**	**73.62%**
2	49.44	**48.78**	15.88	**15.87**	**67.45%**
3	77.25	**76.57**	47.13	**41.75**	**45.47%**
4	86.68	**86.22**	60.11	**57.03**	**33.86%**
5	117.59	**116.37**	104.38	**96.10**	**17.42%**

Table 2: Power-Consumption Comparison between FPVC and VPVC

4 Conclusion

From the results of experimentation, it is clear that VPVC is an efficient control method for a multi-axis hydraulic actuation system compared with a traditional industrial fixed supply pressure system. The dynamic performance of VPVC is satisfactory as well, but this is reliant on a highly responsive servomotor. For further improvement, some research on refined feedback control should be carried out, to get a better position tracking.

Nomenclature

Variable	*Description*	*Unit*
P_S	*Supply pressure*	*[bar]*
P_{SO}	*Predicted pressure required with fully open valve*	*[bar]*
P_{SC}	*Predicted pressure required to avoid cavitation*	*[bar]*
P_R	*Return pressure*	*[bar]*
P_{th}	*Threshold pressure to avoid cavitation*	*[bar]*
x	*Spool opening of modulating valve*	
α	*Area ratio of unequal area cylinder (large area / small area)*	
q	*Generalized force for desired motion*	
I	*Inertia*	*[kgm^2]*
M	*Mass of components to robotic arm*	*[kg]*
MA	*Master actuator*	

References

/1/ R. Finzel and S. Helduser. Energy-Efficient Electro-Hydraulic Control Systems for Mobile Machinery / Flow Matching. In: *6th International Fluid Power Conference*. Dresden. 2008.

/2/ Djurovic, M. and Helduser, S. New Control Strategies for Electrohydraulic Load-Sensing. Power Transmission and Motion Control (PTMC), Bath, 2004.

/3/ Rico. H. Hansen, Torben. O. Andersen and Henrik. C. Pedersen. Development and Implementation of an Advanced Power Management Algorithm for Electronic Load Sensing on a Telehandler. Fluid Power and Motion Control (FPMC), Bath, 2010.

/4/ Marco Scopesi, Prof. Andrew Plummer and Can Du. Energy Efficient Variable Pressure Valve-controlled Hydraulic Actuation. In: *Dynamic Systems and Control Conference (DSCC) / Fluid Power and Motion Control (FPMC)*, Arlington, 2011.